

Seeded Induction Period and Secondary Nucleation of Lithium Carbonate

SUN Yu-zhu(孙玉柱), SONG Xing-fu(宋兴福), WANG Jin(汪瑾), LUO Yan(罗妍), YU Jian-guo(于建国)

(National Engineering Research Center for Integrated Utilization of Salt Lake Resources,
East China University of Science and Technology, Shanghai 200237, China)

Abstract: Seeded nucleation of lithium carbonate in aqueous solution during reactive crystallization was monitored by FBRM (focused beam reflectance measurement) and PVM (particle video microscope). The impacts of operating variables, such as seed size and loading, stirring speed, on induction period and secondary nucleation were investigated and explained by an adsorption model. The results show that seed surface area plays an important role in secondary nucleation, for more surface area has higher adsorption capacity and consumes more supersaturation on seed growth, thus restrains nucleation better. A method through comparison between pure breakage/attrition and nucleation process was put forward to distinguish attrition-induced and surface-induced nucleations quantitatively, which can reveal the contributions of different nucleation mechanisms. The nucleation processes in different conditions were studied, the principles and valuable experimental data were obtained for seeding approach primarily. FBRM and PVM are useful on-line apparatuses to facilitate seed selection and seeding optimization.

Key words: lithium carbonate; reactive crystallization; secondary nucleation; focused beam reflectance measurement; particle video microscope

CLC No.: TQ028.5

Document Code: A

Article ID: 1009-606X(2009)04-0652-09

1 INTRODUCTION

Nucleation can be classified as primary and secondary nucleations. The former is spontaneous nucleations in a bulk solution when the supersaturation reaches a critical degree. While under lower supersaturation, nucleation can be induced only by the introduction of seeds, such type is the so called secondary nucleation. Since most practical crystallization processes are operated in the presence of seed, so secondary nucleation has been recognized as the dominant mechanism of nucleation in a suspension crystallizer and attracted much attention and research. Mullin^[1], Randolph et al.^[2], Myerson^[3] and Ding et al.^[4] have made reviews on this subject.

Induction period is closely related to the metastable zone width and nucleation rate, many efforts have been devoted to this field. However, due to lacking of suitable apparatus with high sensitivity and accuracy, the studies on seeded induction period are not as sufficient as those on unseeded cases, though seeded induction period can provide valuable information on the secondary nucleation and seeding methodology. Mullin^[1] pointed out that the presence of seed crystals generally reduced the induction period, but did not

necessarily eliminate it. Recently, Tai et al.^[5] studied the effect of seed on the induction period in $\text{CaCl}_2\text{-Na}_2\text{CO}_3$ system, Kim et al.^[6] studied the effects of initial precipitates on the induction period of L-ornithine-L-aspartate during semi-batch drowning out crystallization, but they only used one kind of seed.

FBRM (focused beam reflectance measurement, Mettler Toledo, USA) is an on-line apparatus that can directly monitor CLD (chord length distribution) every 2 s, so it is a useful and effective equipment in detection of nucleation^[7,8], for it can record rich information all the way during crystallization without sampling, such as nucleation, growth, agglomeration, breakage and ripening. The principle about FBRM can be referred to relative literatures^[9,10]. PVM (particle video microscope, Mettler Toledo, USA) is an on-line crystal image analysis apparatus that can take 10 photos per second, monitoring shape of crystals in an intuitional and detailed way. Therefore, the main aim of this work is to study the effects and mechanism of seed size (LC), seed loading (SL) and other operating variables on seeded induction period and nucleation rate of Li_2CO_3 using FBRM and PVM, to get better insight into the secondary nucleation and obtain valuable experimental data for the optimization of seeding approach.

Received date: 2009-03-09; Accepted date: 2009-05-08

Foundation item: Supported by Shanghai Leading Academic Discipline Project (No.B506); Program for New Century Excellent Talents in University (No. NCET-08-0776)

Biography: SUN Yu-zhu(1979-), male, native of Tangshan City, Hebei Province, doctoral student, major in chemical engineering; SONG Xing-fu, corresponding author, Tel: 021-64252170, E-mail: xfsong@ecust.edu.cn.

2 THEORY

On the basis of summerization and improvement of previous researches^[1-4,11-15], an adsorption model was described in this study to explain seeded nucleation process. In the supersaturated solution, there are numerous rapid moving molecules and ions, clusters and embryos, they can be called by a joint name—nucleic element. When a crystal seed is introduced into the supersaturated solution, due to the attraction of electrostatic force and Van der Waals force, the nucleic element in the bulk solution will be absorbed to the surface of seed, forming a adsorption layer, thus,

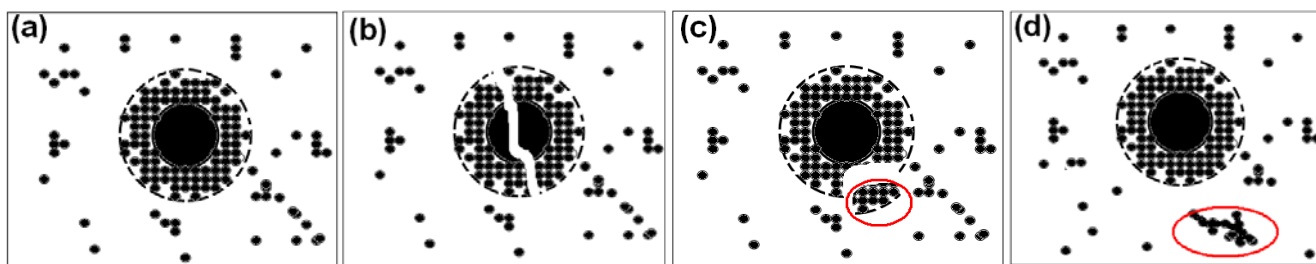


Fig.1 Schematic diagram of adsorption model

Mersmann et al.^[11,12] splitted up the secondary nucleation rate B_{sec} into two contributions, because these two mechanisms are quite different:

$$B_{\text{sec}} = B_{\text{att}} + B_{\text{surf}},$$

where B_{att} is the attrition-induced nucleation rate, B_{surf} the surface-induced nucleation rate. The total nucleation rate B is given by

$$B = B_{\text{hom}} + B_{\text{het}} + B_{\text{att}} + B_{\text{surf}},$$

where B_{hom} is the homogeneous primary nucleation rate, and B_{het} the heterogeneous primary nucleation rate. One of these four nucleation mechanisms is dominant in different supersaturation ranges, at high supersaturation, nucleation mechanism is likely to change from a primary heterogeneous or secondary mechanism to a homogeneous one.

Tai et al.^[13] put forward the concept of interfacial supersaturation, they postulated that the number of nuclei which survive in the bulk was determined by the overall supersaturation, but the number of nuclei generated by contact was influenced by the interfacial supersaturation. In the interfacial phase, for the molecules, ions or clusters, the nucleation free energy is lower than that in the bulk solution, as for the embryos, the adsorption creates a high concentration of embryos and promotes them coagulating rapidly and producing

three phases take shape [see Fig.1(a)], crystal solid phase, interfacial phase and liquid phase, so the nuclei originate from one of the above phases.

Case 1. From crystal solid phase, seed may generate fragments because of breakage and attrition [see Fig.1(b)].

Case 2. From interfacial phase, there is the main mechanism of secondary nucleation, which will be discussed detailedly later [see Fig.1(c)].

Case 3. From liquid phase, if the supersaturation is very high, the spontaneous nucleation may occur [see Fig.1(d)].

particles larger than the critical nuclei^[14,15]. In a word, nucleation is much easier in the interfacial phase than in the bulk solution. The interfacial phase is a loose layer including molecules, ions, clusters, embryos, and nuclei, some of which will be built into the crystal body, the others will be swept out due to fluid shear or collision and become secondary nuclei.

To some extent, seed can be regarded as sorbent in the supersaturated solution, its adsorption quantity is directly related to its surface area, so for a given supersaturation, only when the seed loading exceeds a certain value, can they lower the interfacial and bulk supersaturation to a critical level to avoid burst nucleation.

3 EXPERIMENTAL

3.1 Materials and Apparatus

LiCl-H₂O (AR, Sinopharm Chemical Reagent Co., Ltd.), anhydrous Na₂CO₃ (AR, Shanghai Hongguang Chemicals Factory). The solutions were prepared with deionized water and filtered by 3 μm (pore size) membrane. The concentrations were determined by ion chromatogram (Metrohm, Switzerland). A series of seeds were prepared through sieving Li₂CO₃ crystals (AR, Sinopharm Chemical Reagent Co., Ltd.), 1[#], 3[#] and 5[#] seed, 401, 225 and 21 μm (volume mean crystal size, measured by Malvern, Mastersizer 2000, UK)

respectively, were used in this study.

Figure 2 presents the schematic diagram of experimental setup. The crystallizer is a 150 mL jacketed glass vessel with an internal diameter 45 mm, the temperature was controlled by a water bath (DC2006, Shanghai Hengping Apparatus Factory) with an accuracy of 0.1 K. A magnetic stirrer is adopted to ensure good mixing. The model of FBRM is S400, in order to get enough and good information on the rapid nucleation process, the main measurement parameters were set as follows: measurement speed 2 m/s, duration 2 s, no time averaging, no weighted chord length. When observing crystals shape, PVM probe was inserted in the solution like that of FBRM.

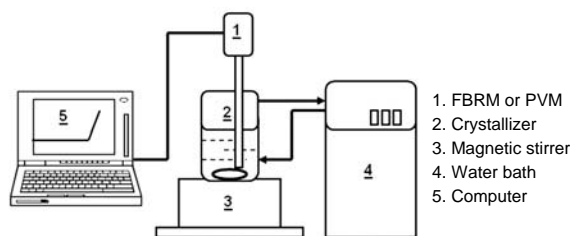


Fig.2 Schematic diagram of experiment setup

3.2 Procedure

Firstly, 4.145 mol/L LiCl 40 mL solution was introduced in the crystallizer, FBRM probe immersed in

the solution near the stirring rod to monitor the chord length distribution (CLD), and then the circulation of water bath and agitation initiated. When the solution temperature was stabilized, rapidly a quantity of 1.001 mol/L Na_2CO_3 solution and seeds was added, the sharp rise of total crystal number indicated that nucleation occurred. Not only the induction period, but also the nucleation rate and crystal growth rate could be achieved simultaneously.

4 RESULTS AND DISCUSSION

4.1 Analysis on Seeded Crystallization Processes

Experimental results show that 1[#] and 3[#] seed have similar impact on the seeded nucleation, for the sake of convenience, only the process with 3[#] seed is analyzed here and hereinafter sometimes. In Fig.3(a), the chord length distribution (CLD) of 3[#] seed is bimodal, the left convexity is related to small particles (<50 μm), and the other to large particles (>50 μm). From 0 to 40 s, the right convexity has nearly no change, whereas the left convexity rises up, especially the part less than 10 μm . The explosive nucleation begins at 40 s, since that time, the left convexity goes up drastically, the CLD gradually changes to unimodal for the emergence of numerous nuclei (S_L is the seed mass, and N_p stirring speed).

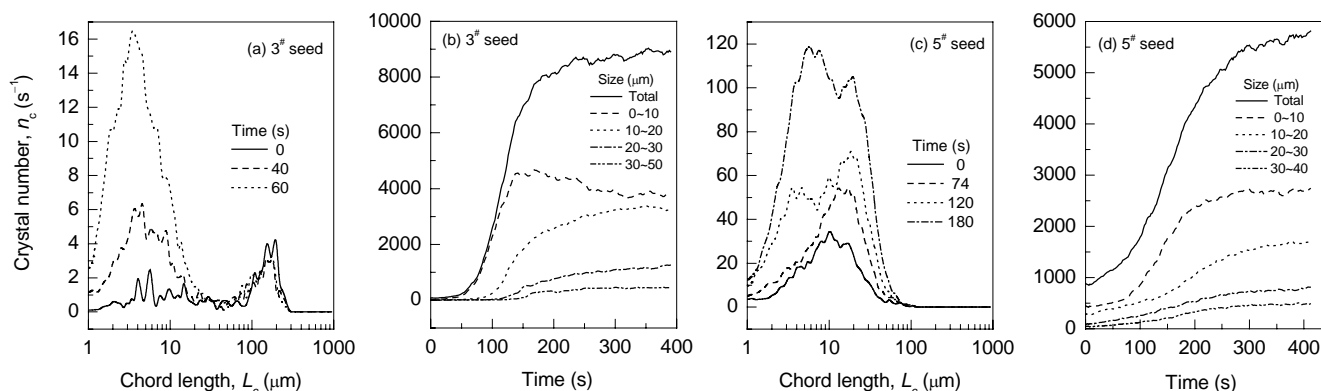


Fig.3 On-line monitoring of seeded nucleation ($S=3.4$, $S_L=0.75$ g/L, $N_p=500$ r/min, 293 K)

But nucleation with 5[#] seed is different. As seen in Fig.3(c), from 0 to 74 s, the CLD with 5[#] seed is unimodal, and gradually shifts to the right side, indicating that supersaturation was mainly consumed by seeds growth. After 74 s, the part less than 10 μm rises up rapidly, the CLD changes to bimodal. The left convexity represents the newly produced nuclei, which goes up persistently, the right convexity represents the original seeds, which moves to the right direction, suggesting the growth of seeds. It is interesting to point

out that the chord length range of nuclei monitored by FBRM is mainly between 0 and 10 μm , and the median chord length of the nuclei is about 5 μm , whether in primary or seeded nucleation. So the main characteristic of explosive nucleation in this system is the persistent drastic rise of nuclei less than 10 μm .

It should be noted that the nucleation rate of Li_2CO_3 is very rapid, without FBRM, we would not have measured the transient CLD. It is nearly impossible to take out dozens of samples without any

damage and measure them accurately within just 1 min.

4.2 Induction Period

4.2.1 Determination of induction period

Theoretically, the sharp rise of total chord number (N_c) indicates nucleation, but experimental results show that the evolution of total chord counts is a continuous curve presenting a gradual increase at the beginning of nucleation stage, not a strictly sudden step change (see Fig.4), Kind et al.^[16] reported the similar result. Furthermore, the total chord counts increases from the start. So strictly speaking, secondary nucleation begins at the commencement (even only one crystal has increased), it is nearly impossible that the crystal number has no change due to the collision and attrition of seeds in the stirred fluid field together with the presence of supersaturation. Thus, there was no rigorous induction period (sudden birth of nuclei) after introduction of seed in this experiment.

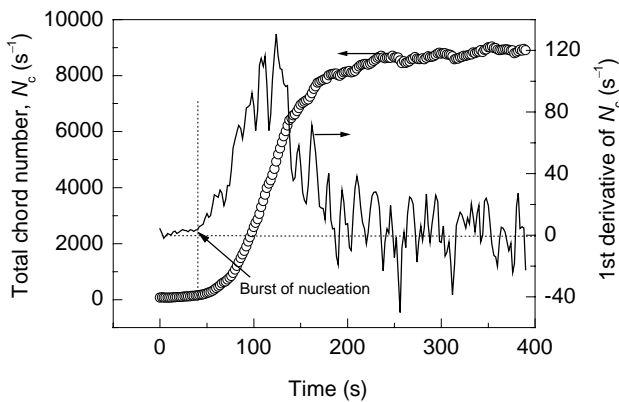


Fig.4 Evolution of total chord counts and apparent nucleation rate ($S=3.4$, 3[#] seed, $S_L=0.75$ g/L, $N_p=500$ r/min, 293 K)

On the other hand, as shown in Fig.4, the increase of total chord counts in the initial stage is very slow,

which can be ignored, compared with the so called burst nucleation. Consequently, the first stage can be regarded as the induction period. Besides, induction period is always connected with nucleation and growth, Mersmann et al.^[12] pointed that the various definitions with different metastable limits were based on nucleation rate, once it exceeded a certain value. Similarly, the determination of induction period should also be based on a certain nucleation rate. Generally, the main intention of introducing seed is to avoid or restrain explosive nucleation, so the burst of nucleation is regarded as the end of induction period in this work. FBRM can directly gives the evolution of apparent nucleation rate using the first derivation calculus of the total chord counts, the interval between the start and the sharp rise of apparent nucleation rate is the induction period. It is clear that the apparent nucleation rate firstly increases, for the newly produced nuclei also induce contact nucleation, and then drops down due to the decrease of supersaturation, at last it fluctuates around zero.

4.2.2 Impacts of operating variables on induction period

The impacts of operating variables on induction period are shown in Fig.5, because the induction is so closely connected with nucleation, for the sake of concision, only the results are given here. From Fig.5 we can see that with the increase of supersaturation (S), the induction period drops down obviously, with the same amount of seed, the decrease of seed size postpones the induction period, with the increase of seed mass (S_L), the induction periods of supersaturated solution with 1[#] and 3[#] seed decrease, whereas that with 5[#] seed rises up, the increase of stirring speed (N_p) leads to slight reduction in the induction period.

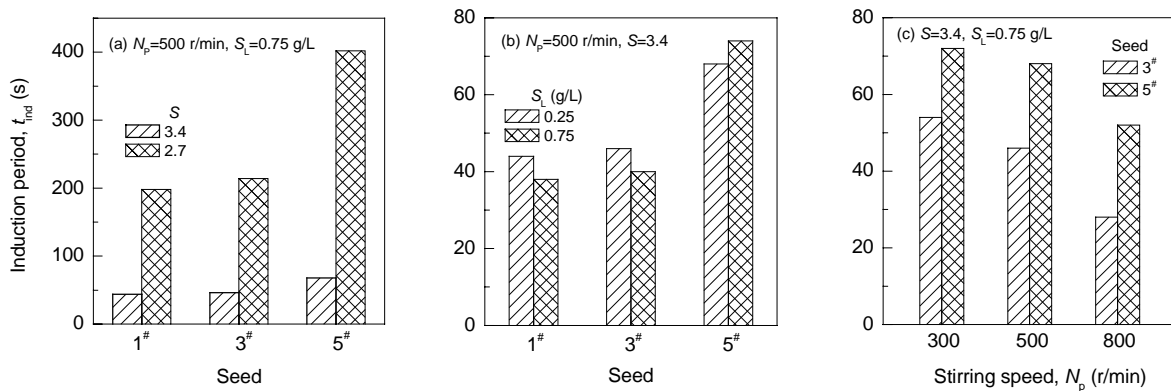


Fig.5 Impacts of operating variables on induction period (293 K)

4.2.3 Distinguishing between attrition-induced and surface-induced nucleations

Mersmann et al.^[12] indicated that there was no experimental way to distinguish the attrition-induced

nucleation and surface-induced nucleation, or even quantify these two sources of secondary nucleation. In order to make out either attrition-induced or surface-induced nucleation causes the slight increase of total chord counts in the induction period, a method through comparison between pure breakage/attrition and nucleation process was put forward to distinguish and quantify them. The same amount of seeds as that in supersaturated aqueous solution was stirred in ethanol ($S_L=0.75$ g/L, $N_p=500$ r/min, 293 K), the CLD was

monitored by FBRM, because Li_2CO_3 did not dissolve in ethanol, so the increase of crystal number revealed the attrition-induced nucleation solely. As shown in Fig.6(a) and Fig.6(b), breakage and attrition of 3[#] seed are very obvious, because large seeds have greater collision probabilities, generating more nuclei, whereas the CLD of 5[#] seed has nearly no change [see Fig.6(c) and Fig.6(d)], for small seeds may flow along streamline within the turbulent eddies, rarely collide to each other, stirring rod or the crystallizer wall.

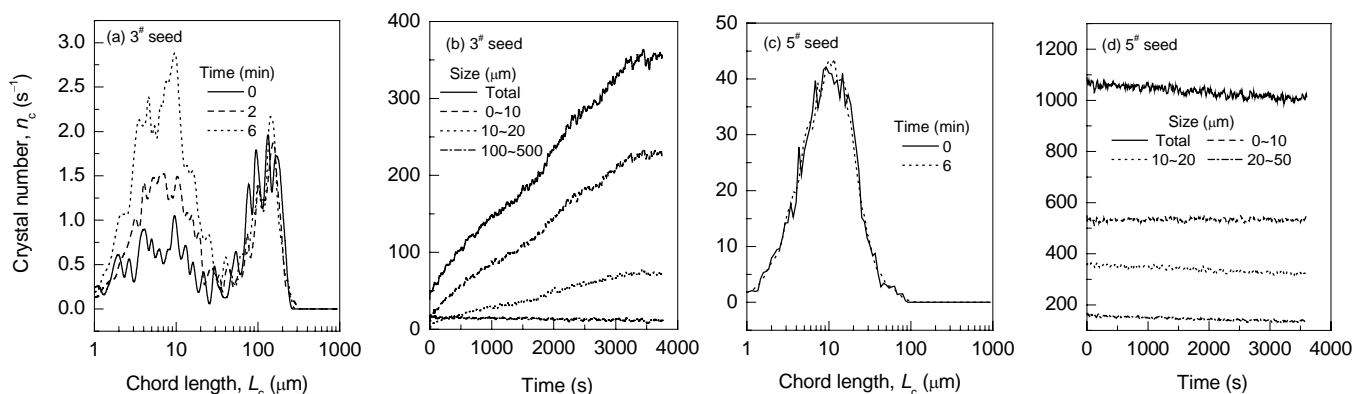


Fig.6 Breakage and attrition of seeds ($S_L=0.75$ g/L, $N_p=500$ r/min, 293 K)

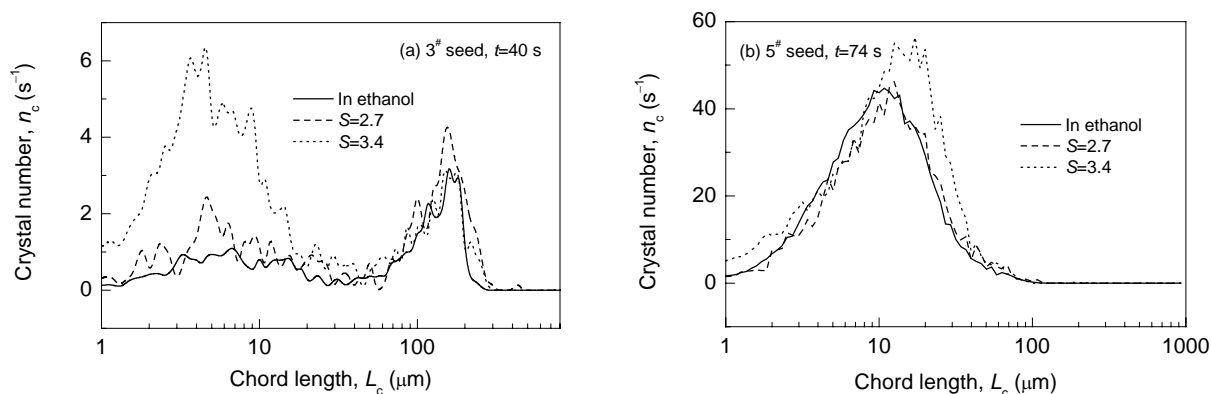


Fig.7 Comparison of chord length distributions in supersaturated solution and ethanol

Figure 7(a) shows the comparison of chord length distributions of 3[#] seed in supersaturated aqueous solution and ethanol at $t=40$ s, the curve at $S=2.7$ is close to that in ethanol, while the curve at $S=3.4$ is above to them, demonstrating that attrition nucleation is the main mechanism at low supersaturation, while at high supersaturation, besides attrition nucleation, surface nucleation also occurs. Fig.7(b) shows the similar comparison of 5[#] seed at $t=74$ s, as mentioned above, stirring causes nearly no change on CLD of 5[#] seed, so the slight increase of chord number almost totally originates from weak surface nucleation. Therefore, the increase of the total chord counts of 3[#] seed in the

induction period includes both attrition-induced nucleation and surface-induced nucleation, while that of 5[#] seed nearly only involves surface-induced nucleation. As seen, though under the same supersaturation, the nucleation mechanism is not identical, which not only is related to supersaturation, but also to seed properties, especially the seed size and surface area.

4.2.4 On-line image observation by PVM

The shape of seeds can be monitored by PVM during the reactive crystallization. Fig.8 gives the typical observation, which shows the shape of 5[#] seed at different times. From 0 to 60 s, the seeds gradually grow up and aggregate to some extent, a few new nuclei can

be seen, while at $t=90$ s, the burst of nucleation results in a great number of nuclei (the small spots represent the newly generated nuclei) against the growing seeds. Though the resolution of PVM is not as high as SEM and AFM, but its advantages are obvious, it can record

the crystal shape of bulk particles in turbulent fluid in real production equipment, while optical microscope, SEM and AFM are not fit to that, but can not record the transient crystal image as quickly as PVM.

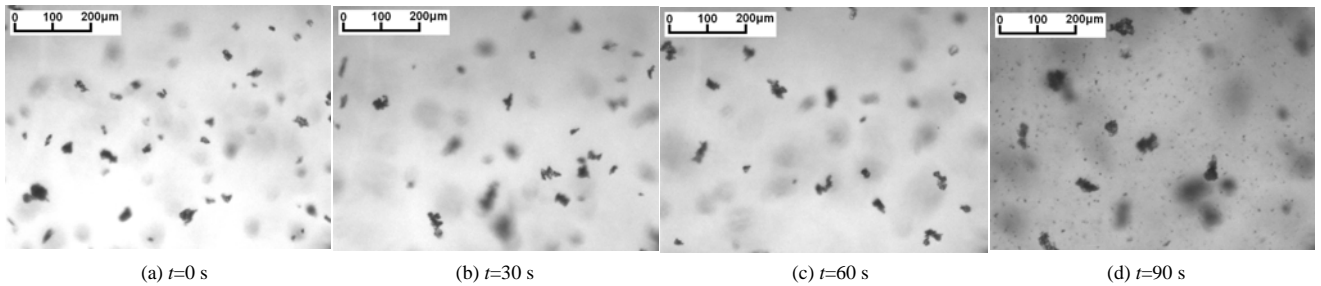


Fig.8 PVM images of 5[#] seed at different times ($S=3.4$, $S_L=0.75$ g/L, $N_p=500$ r/min, 293 K)

4.2.5 Comparison between secondary nucleation and heterogeneous nucleation

Heterogeneous primary nucleation was studied through adding coal fly ash to the crystallization process as the foreign particles. Fig.9 shows that both the fly coal ash and seed reduce the induction period, but the induction period with seed is much less than that with

coal fly ash, meaning that solution in the presence of seed is more readily to nucleation than that with heteronuclei. This is because seed is just the crystallizing substance, with the identical crystal lattice, so the solute is much easier to be adsorbed onto the crystal surface.

4.3 Impacts of Operating Variables on Nucleation

4.3.1 Effect of supersaturation

Figure 10(a) shows that the nucleation at $S=3.4$ is much rapider than that at 2.7, for supersaturation is the direct driving force of nucleation and crystal growth. Though the introduction of seed must induce nucleation in the initial period, but as for the whole crystallization, seed may facilitate or restrain nucleation compared with the unseeded cases depending on experimental conditions. If the supersaturation is relatively high, such as at 3.4, seed facilitates nucleation like catalyst, whether which seed was added [see Fig.10(b)].

4.3.2 Effect of seed size

Figure 10(a) shows the impact of seed size on nucleation, with the same amount of seed, 1[#] and 3[#] seeds have the similar effect, while the nucleation rate with 5[#] seed is much slow, suggesting that seed surface

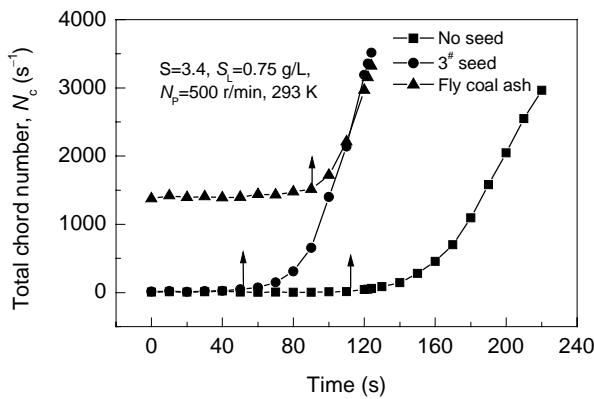


Fig.9 Comparison between secondary nucleation and heterogeneous nucleation

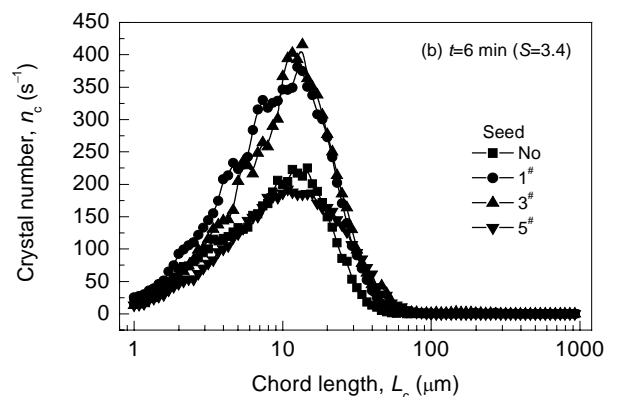
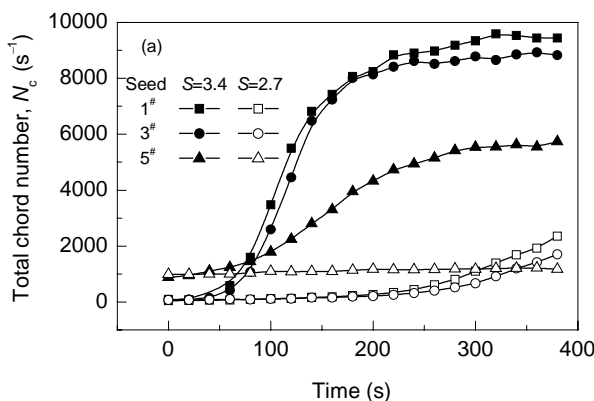


Fig.10 Effect of supersaturation on nucleation ($S_L=0.75$ g/L, $N_p=500$ r/min, 293 K)

area plays an important role in secondary nucleation. It is known that supersaturation is consumed by either nucleation or crystal growth, with the same amount of seeds, the smaller seeds have larger surface area, on one hand, they have higher absorption capacity, can absorb much more solute, thus reduce both the bulk and interfacial supersaturation, on the other hand, they can provide more growth positions and consume more supersaturation on crystal growth, thus restrain nucleation better.

The evolution of mean size (see Fig.11) also gives

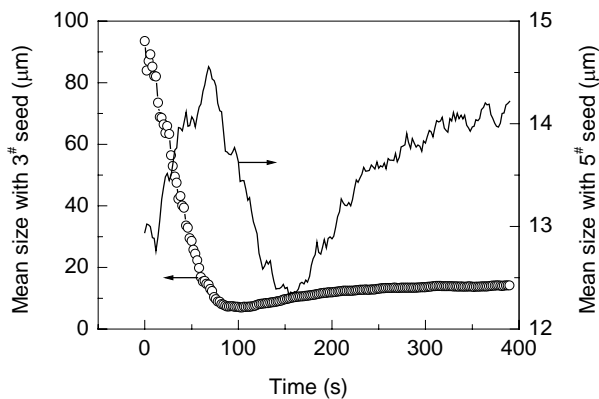


Fig.11 Evolution of mean chord length size

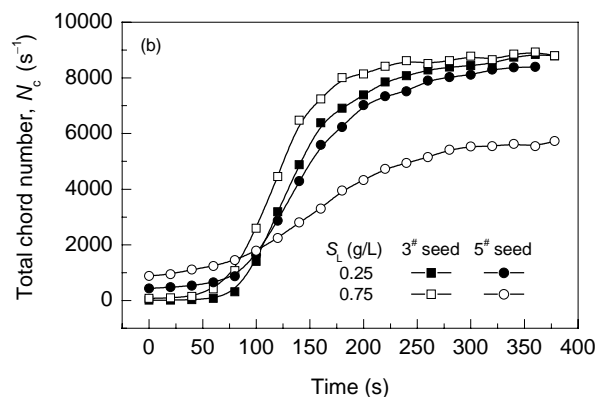
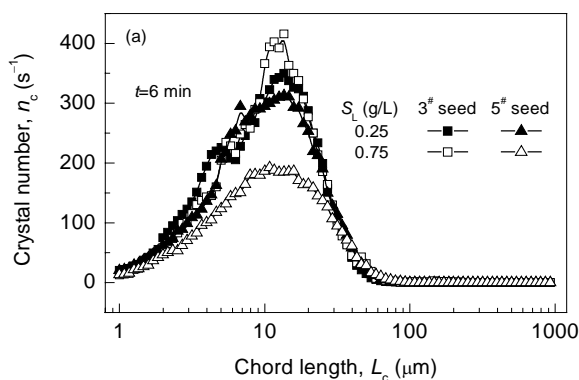


Fig.12 Effect of seed load on nucleation ($S=3.4$, $N_p=500$ r/min, 293 K)

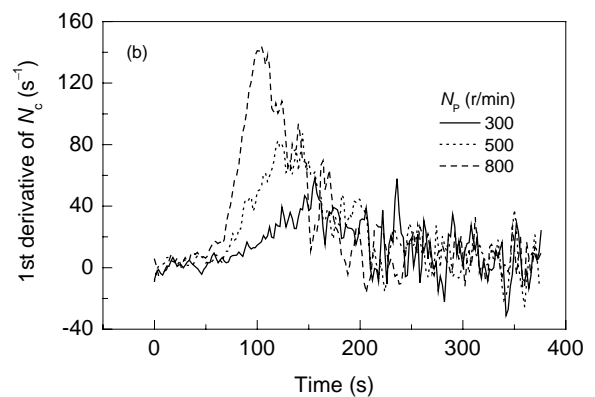
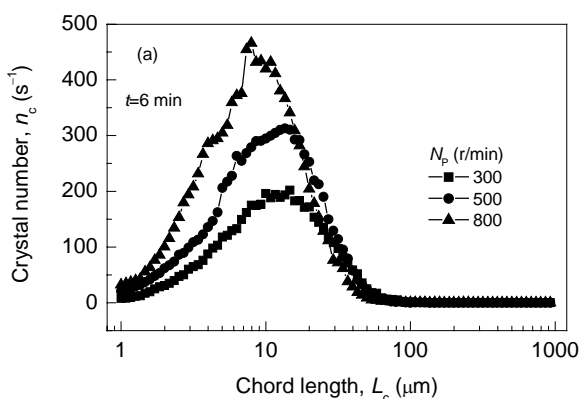


Fig.13 Effect of stirring speed on nucleation ($S=3.4$, 5# seed, $S_L=0.75$ g/L, 293 K)

interesting information. Because of breakage and attrition of large particles and consecutive nucleation, the mean crystal size of crystallization with 3# seed decreases monotonously in the initial period, and then increases slightly due to crystal growth; whereas that with 5# seed firstly increases for the seeds growth, and then drops down for the considerable nucleation, the turning point is basically corresponding to the burst nucleation time, of course, crystal growth also causes increases of the mean size eventually.

4.3.3 Effect of seed loading

Figure 12 shows that the increase of 3# seed loading causes earlier and faster nucleation, because in spite of such a quantity increase, the seed surface area is still small and does not cause obvious reduction on supersaturation. Additionally, more larger seeds are easier to collide and produce more contact nuclei. Whereas the increase of 5# seed loading decreases the nucleation rate obviously, thus the more seed surface area absorbs and consumes more supersaturation.

4.3.4 Effect of stirring speed

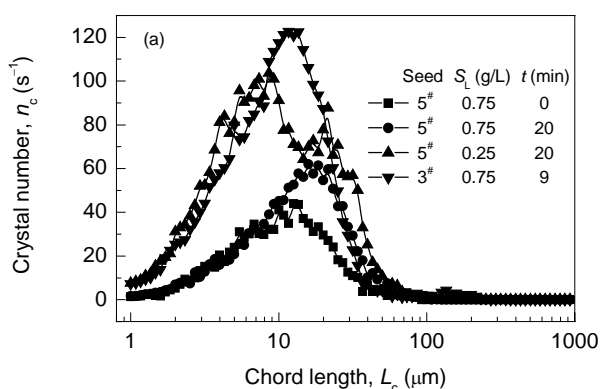
The stirring speed varies at 300, 500 and 800 r/min, whether which seed is added, the higher stirring speed leads to much more nuclei and smaller mean crystal size, for the higher stirring speed intensifies the fluid shear

and seeds collision, strengthening both the attrition and surface nucleation, thus produce more nuclei (Fig.13).

4.4 Analysis on Seed Application

4.4.1 Elimination of burst nucleation through seeding

In this research, the characteristic of burst nucleation is the rapid consecutive rise of small nuclei less than 10 μm . It is found that in such experimental conditions ($S=2.7$, 5[#] seed, $S_L \geq 0.75$ g/L, 293 K), burst nucleation does not occur. As seen in Fig.14(a), the chord length distribution shifts to the right from start to



the end, small nuclei do not rise up at all, meaning that supersaturation is chiefly consumed by crystal growth, and the surface nucleation is slight, it is just the expected result in industrial crystallization. Comparably, the less seed loading or larger seed size at the same supersaturation can not obtain such good effect, causing burst nucleation still [see Fig.14(b)], because they do not have sufficient adsorption capacity to lower the supersaturation under a critical level to avoid burst nucleation.

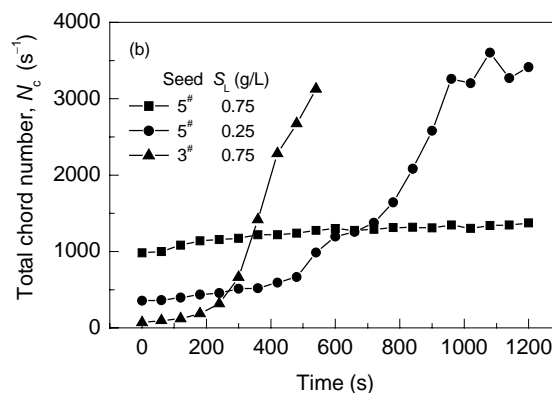


Fig.14 Effects of different operating variables on chord length distribution and nucleation ($N_p=500$ r/min, 293 K)

4.4.2 Basic methods of seeding strategy

Through the above analysis we can see that the impacts of seed on nucleation are very complicated, so when optimizing the seeding strategy, seed size, seed loading, supersaturation level, fluid field, etc., should be taken into consideration. According to the theory of secondary nucleation and experimental results of this study, seeding strategy should pay great attention to the following aspects:

Firstly, making out which nucleation mechanism is dominant at different supersaturation levels. Supersaturation is the key factor influencing nucleation, if supersaturation level is high (for this study, when $S \geq 3.4$, 293 K), spontaneous nucleation will occur and no seed can suppress it.

Secondly, determining contributions of different nucleation mechanisms under various conditions. For the big seed (1[#] and 3[#] seeds), attrition-induced nucleation may play an important role, while for the small seed (5[#] seed), almost all nuclei from surface-induced nucleation.

Thirdly, exploring the effects of seed on product quality. The multi-objectives of seeding may include large mean crystal size, narrow distribution, high purity product and so on, the experimental results show that 5[#] seed is better than 1[#] and 3[#] seeds in this system.

Fourthly, determining the least seed loading to

avoid explosive nucleation, for instance, when introducing 5[#] seed (293 K, $S=2.7$), the least seed loading is 0.75 g/L.

5 CONCLUSIONS

The seeded nucleation of Li_2CO_3 during reactive crystallization was monitored by FBRM and PVM, the impacts of operating variables on seeded induction period and secondary nucleation rate were investigated. Adsorption model provides good explanation for the experimentally observed secondary nucleation phenomenon.

A method through comparison between pure breakage/attrition and nucleation was put forward to distinguish attrition-induced and surface-induced nucleations quantitatively, which can reveal the contributions of different nucleation mechanisms under various conditions. The results show that nucleation mechanism is not only related to supersaturation, but also to seed properties, especially the seed surface area.

The nucleation processes under different conditions were studied, obtaining the principles and valuable experimental data for seeding approach primarily. The results show that the seed surface area plays a very important role in the secondary nucleation, for more surface area has higher adsorption capacity and consumes more supersaturation on seed growth, thus

restrain nucleation better, so 5[#] seed is better than 1[#] and 3[#] seeds. As on-line apparatuses, FBRM and PVM can facilitate seed selection and optimization of seeding strategy, and speed up the engineering development.

REFERENCES:

- [1] Mullin J W. Crystallization, 3rd Ed. [M]. Oxford: Butterworth Heinemann Press, 1992. 185–189.
- [2] Randolph A D, Larson M A. Theory of Particulate Processes, 2nd Ed. [M]. San Diego: Academic Press Inc., 1988. 123–128.
- [3] Myerson A S. Handbook of Industrial Crystallization, 2nd Ed. [M]. Oxford: Butterworth Heinemann Press, 2002. 46–50.
- [4] Ding X H, Tan Q. Industrial Crystallization [M]. Beijing: Chemical Industry Press, 1985. 81–89 (in Chinese).
- [5] Tai C Y, Chien W C. Interpreting the Effects of Operating Variables on the Induction Period of CaCl₂-Na₂CO₃ System by a Cluster Coagulation Model [J]. Chem. Eng. Sci., 2003, 58(14): 3233–3241.
- [6] Kim Y, Hyung W, Haam S, et al. The Effect of Initial Precipitates on the Induction Period of L-Prothine-L-aspartate during Semi-batch Drowning out Crystallization [J]. J. Cryst. Growth, 2006, 289(1): 236–244.
- [7] Barrett P, Glennon B. Characterizing the Metastable Zone Width and Solubility Curve Using Lasentec FBRM and PVM [J]. Chem. Eng. Res. Des., 2002, 80(7): 799–805.
- [8] Fujiwara M, Chow P S, Ma D L, et al. Paracetamol Crystallization Using Laser Back Scattering and ATR-FTIR Spectroscopy: Metastability, Agglomeration and Control [J]. Cryst. Growth Des., 2002, 2(5): 363–370.
- [9] Sparks R G, Dobbs C L. The Use of Laser Back Scatter Instrument at Ion for the On-line Measurement of Particle Size Distribution for Emulsions [J] Part. Part. Sys. Char., 1993, 10(5): 279–289 .
- [10] Ruf A, Worlitschec J, Mazzotti M. Modeling and Experimental Analysis of PSD Measurements through FBRM [J]. Part. Part. Sys. Char., 2000, 17(4): 167–179.
- [11] Mersmann A. Supersaturation and Nucleation [J]. Trans. IChemE, Part A, 1996, 74: 812–819.
- [12] Mersmann A, Bartosch K. How to Predict the Metastable Zone [J]. J. Cryst. Growth, 1998, 183(1/2): 240–250.
- [13] Tai C Y, Wu J F, Rousseau R W J. Interfacial Supersaturation Crystal Growth, Secondary Nucleation, and Crystal Growth [J]. J. Cryst. Growth, 1992, 116(3/4): 294–306.
- [14] Qian R Y, Botsaris G D. A New Mechanism for Nuclei Formation in Suspension Crystallizers: The Role of Interparticle Forces [J]. Chem. Eng. Sci., 1997, 52(20): 3229–3240.
- [15] Qian R Y, Botsaris G D. Nuclei Breeding from a Chiral Crystal Seed of NaClO₃ [J]. Chem. Eng. Sci., 1998, 53(9): 1745–1756.
- [16] Kind M, Mersmann A. On Supersaturation during Mass Crystallization from Solution [J]. Chem. Eng. Technol., 1990, 13(1): 50–62.